

# Parameterization of Real-Time 3D Speckle Tracking Framework for Cardiac Strain Assessment

Auranuch Lorsakul, *Student Member, IEEE*, Qi Duan, *Member, IEEE*, Ming Jack Po, *Student Member, IEEE*, Elsa Angelini, *Member, IEEE*, Shunichi Homma, and Andrew F. Laine, *Fellow, IEEE*

**Abstract**—Cross-correlation based 3D speckle tracking algorithm can be used to automatically track myocardial motion on three dimensional real-time (RT3D) echocardiography. The goal of this study was to experimentally investigate the effects of different parameters associated with such algorithm to ensure accurate cardiac strain measurements. The investigation was performed on 10 chronic obstructive pulmonary disease RT3DE cardiac ultrasound images. The following two parameters were investigated: 1) the gradient threshold of the anisotropic diffusion pre-filtering and 2) the window size of the cross correlation template matching in the speckle tracking. Results suggest that the optimal gradient threshold of the anisotropic filter depends on the average gradient of the background speckle noise, and that an optimal pair of template size and search window size can be identified determines the cross-correlation level and computational cost.

## I. INTRODUCTION

CARDIOVASCULAR diseases such as myocardial infarction (MI or heart attack) are the current leading causes of mortality, morbidity and rising healthcare costs in the United States [1]. Advances in imaging technologies such as the development of real-time three-dimensional (RT3D) echocardiography are expected to improve the clinical assessment and management of these cardiovascular pathologies. Several vendors have recently released RT3D ultrasound systems, including GE's Vivid 7 and E9, Siemens' SC2000, Toshiba's Artida, Philips' SONOS 7500 and iE33 Systems. However, few of these machines currently provide image analysis tools that fully leverage the true potential of RT3DE data. For example, many of the machines continue to calculate strain measurements using 2D computations.

Quantitative evaluation of 3D regional motion enables to assess regional strain and dyssynchrony that are currently impossible to estimate non-invasively. A number of studies have used 3D speckle tracking algorithms to extract myocardial strain measurements using RT3D ultrasound data [2-5].

Manuscript received June 20, 2011. This work was funded by the American Heart Association grant #0640005N, NIH 1R01HL085160-01A2, and NIH/NHLBI 1R01HL086578-01A2.

A. Lorsakul, M. J. Po and A. F. Laine are with Department of Biomedical Engineering, Columbia University, ET-351, 1210 Amsterdam Avenue, New York, NY 10027, USA (phone: 212-854-5996; e-mail: al2776, mp2591, laine@columbia.edu).

Q. Duan is with NINDS, NIH, 10 Center Dr, Bethesda, MD 20892 (e-mail: Qi.Duan@nih.gov).

E. D. Angelini is with Institut Telecom, Department of Image and Signal Processing, Telecom ParisTech, CNRS LTCI, 46 rue Barrault, 75013, Paris, France (e-mail: elsa.angelini@telecom-paristech.fr).

S. Homma is with the Division of Cardiology, Columbia University Medical Center, New York, NY 10027 USA (sh23@columbia.edu).

In previous studies from our group, a speckle tracking algorithm was validated on open chest dog hearts acquired with the Philips iE33 system against strain measurements acquired via sonomicrometry [6-8]. In this study, we investigate this speckle tracking framework on RT3DE data acquired from 10 chronic obstructive pulmonary disease (COPD) patients. This study evaluates the effect of two main parameters in the analysis framework, (1) the non-linear diffusion filtering threshold and (2) the cross-correlation based speckle tracking window and search sizes.

## II. METHODS

### A. Data and Computational Framework

COPD patient recruitment was performed as part of an ongoing MESA study (R01 HL075476) at the Columbia University Medical Center (IRB-AAAD9509). 56 sets of 4D ultrasound datasets were acquired using a Siemens ACUSON SC2000™ with a matrix phased-array called 4Z1c transducer (Siemens, Mountain View, CA). Only the 10 best quality images, selected by the cardiologists, were analyzed in this paper. The acquisitions were ECG gated with the focus depth ranging from 140 to 160 mm and the temporal resolutions ranging from 12 to 15 frames per cardiac cycle.

Using proprietary software tools provided by Siemens AG, we were able to access the raw ultrasound line data in spherical coordinates. The line data was then converted into Cartesian coordinates and interpolated using a fast tri-cubic interpolation algorithm [9]. The reconstructed volumes had spatial resolutions of approximately 0.42-0.77 mm per voxel and a matrix size  $330 \times 330 \times 230$  voxels and intensity range [0, 255]. The reconstructed volumes were analyzed using our cardiac analysis computational framework (Fig. 1).

The left ventricular (LV) myocardial borders were first manually traced on the short axis views at end diastole and then interpolated to generate a binary volume mask. The volumetric images were smoothed by anisotropic diffusion [10], and 3D speckle tracking was then performed to estimate myocardial displacements and consequently compute the local strains.

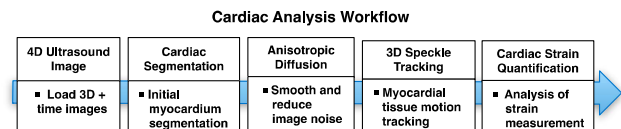


Fig. 1 : Cardiac analysis computational framework for measuring 4D echocardiographic strain.

### B. Parameterization of Anisotropic Diffusion

Anisotropic diffusion, using non-linear 3D filtering, was used to reduce speckle noise and increase image homogeneity before performing motion estimation by speckle tracking [11].

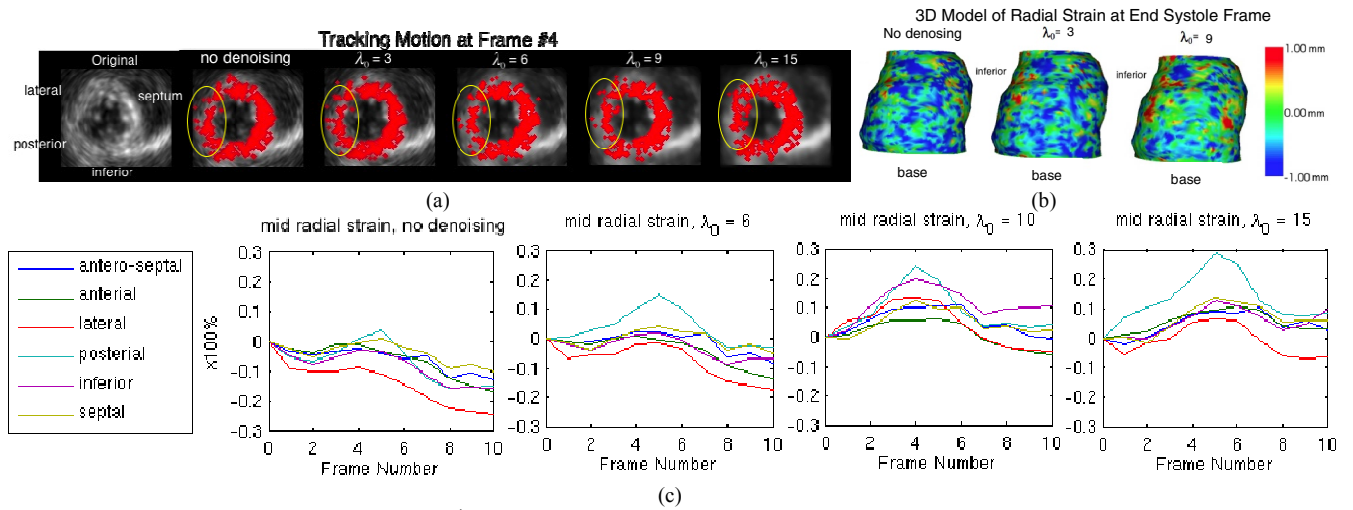


Fig. 2 : (a) Examples of the tracking results at the 4<sup>th</sup> frame after starting the tracking at the 1<sup>st</sup> frame (ED frame) without denoising and with the initial threshold  $\lambda_0 = 3, 6$  and  $15$ , (b) 3D model of radial strain at end systole frame and (c) examples of the temporal profiles of the radial strains at mid LV regions in the systolic phase (contraction) without denoising and with the initial threshold  $\lambda_0 = 6, 10$ , and  $15$ .

Anisotropic diffusion filter is an edge-preserving filter that uses the heat-diffusion equation:

$$\partial_t I = \text{div}(g(|\nabla I(\mathbf{x}, t)|) \cdot \nabla I) \quad (1)$$

$\partial_t$  denotes the temporal derivation,  $I(\mathbf{x}, t)$  the gray levels of a given 3D image dataset at iterative  $t$ ,  $\text{div}$  the divergence and  $\nabla$  the gradient operator. The diffusion function,  $g$ , is typically set to  $g(s) = 1 - \exp[-3.315 / (s / \lambda)^4]$ , where  $s > 0$  and  $g(s) \equiv 1$ , where  $s \equiv 0$ . This equation shows that structures with  $|\nabla I| \gg \lambda$  are regarded as edges where  $g \equiv 0$  [10, 12].

The key parameter of the diffusion process is the *gradient threshold*,  $\lambda$ . On ultrasound textured images, the threshold must decrease with time according to a study proposed by Montagnat *et al* [13] and our group [10]. We proposed in [10] the following linear model to set the gradient weight:

$$\lambda(t) = \lambda_0 + at \quad (2)$$

where  $\lambda_0$  represents an initial gradient value,  $a$  the slope parameter and  $t$  the time iteration index used in the diffusion process. This model enforces the observation that high gradient values are more meaningful as the diffusion process iterates and removes noise components.

### C. Parameterization of 3D Speckle Tracking

For 3D speckle tracking, we used a pointwise 3D template-matching method based on maximizing the cross-correlation coefficient (CC) defined as:

$$CC = \frac{\sum_{\mathbf{x} \in \Omega} (I(\mathbf{x}, t) I(\mathbf{x} + \Delta \mathbf{x}, t + \Delta t))}{\sqrt{\sum_{\mathbf{x} \in \Omega} I^2(\mathbf{x}, t) \sum_{\mathbf{x} \in \Omega} I^2(\mathbf{x} + \Delta \mathbf{x}, t + \Delta t)}} \quad (3)$$

where  $I(\mathbf{x}, t)$  and  $I(\mathbf{x}, t + \Delta t)$  are two consecutive 3D images after the anisotropic diffusion filtering, and  $\Delta \mathbf{x}$  is a displacement a vector.

The key parameters of the 3D speckle tracking are the window size of the template  $\Omega$  and the search range spanned by the template that impact the discriminating power of the CC measure and the accuracy of the displacement. In our framework, each individual point within the myocardium was tracked (approximately  $3.51 - 12.27 \cdot 10^5$  points). After speckle

tracking, cubic smoothing Spline interpolation was performed to remove the high-frequency components of the displacement fields and to smooth the global motion patterns.

### D. Cardiac Strain Assessment

Strain can be computed from the motion field resulting from the speckle tracking. We computed the average segmental radial strains according to the 16-segment model of the LV myocardium prescribed by the American Society of Echocardiography (ASE) [14]. Individual strain components (radial, longitudinal, circumferential) were computed following the method described in [15].

## III. EXPERIMENT AND RESULTS

### A. Anisotropic Diffusion

In this study, we varied the initial gradient threshold  $\lambda_0$  while setting  $a = -1$  [16]. Speckle tracking was performed with and without denoising. For denoising, we set the initial gradient threshold to  $\lambda_0 = 3, 6, 9, 10, 15$  and  $20$ . The segmented binary myocardial mask was used as input to the 3D speckle tracking algorithm. In this experiment, the cross-correlation template matching was performed based on a 7-voxel template and a 9-voxel search.

Tracking results using the different thresholds are illustrated in Fig. 2(a). We can observe that increased anisotropic diffusion (i.e. increasing the threshold value) causes the speckle tracking to provide more uniform displacements in the lateral and posterior segments in Fig. 2(a). The temporal profiles of the radial strains at mid LV regions in the systolic phase are shown in Fig. 2(c) where we can observe that strain increases when anisotropic diffusion increases. The increased strain values were also confirmed on the 3D model at ES in Fig. 2(b). In this example,  $\lambda_0 = 10$  is optimal providing temporal profiles of radial strain of all segments uniform and positive consistent with the systolic phase (expansion) of cardiac cycle.

We further investigated the relationship between the optimal threshold value  $\lambda_0$ , and the background speckle noise level. The experiment was performed by selecting a region of interest at mid level between base and apex, on the ED frame. The average magnitude of the gradient in the background speckle noise in

each dataset was computed and compared to the optimal threshold value  $\lambda_0$ . The results reported in Fig. 3 show that these two values are always very similar.

### B. 3D Speckle Tracking

1) *Cross-Correlation Coefficient*: We investigated the cross correlation values during speckle tracking by varying the template size and the spanned search size, as reported in Table I. The resultant cross-correlation values are displayed in the blue curve in Fig. 4(a). Computational time needed to process one frame using speckle tracking versus template and search sizes are reported in Table I and Fig. 4(b), illustrating that increasing the window size leads to higher computational time.

We also investigated the effects of changing the search size while fixing the template size (3 and 5 voxels). The cross-correlation coefficients were not significantly changed as shown in Fig. 4(a) (red and green curves).

2) *Impact on Strain Measurement*: Ultimately, we investigated the robustness of the derived strain results based on variations in the template and search sizes for the cross-correlation computation. 10 COPD images were denoised using anisotropic diffusion as reported in Table II. Then the cardiac motion was estimated via 3D speckle tracking as described above using two experimental setups: 1) the template size was fixed at 5 voxels while varying the search window size to 7, 9 and 11 voxels and 2) the template size was fixed at 9 voxels while varying the search window size: 9, 11 and 13 voxels. Fig. 5 shows the temporal profiles of the radial strain with a constant denoising parameter,  $\lambda_0 = 10$ , and varying template and search sizes. Mean radial strains in the anterior-septum segments of the 10 data sets in Table II, illustrating the fact that increasing the template size results in higher and fairly consistent strain measurements.

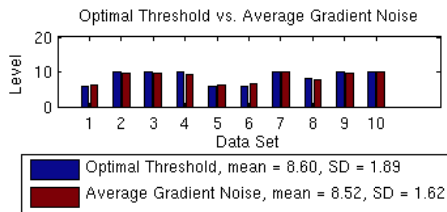


Fig. 3 : Relationship between the optimal threshold values  $\lambda_0$  from Table II and the average magnitudes of the gradient in the background speckle noise of the 10 data sets.

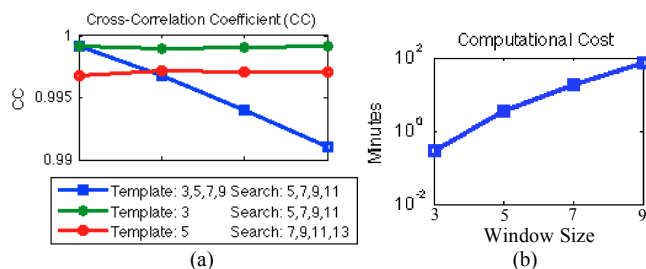


Fig. 4 : (a) Cross-correlation coefficient (CC) as a function of the template size: 3,5,9 with search size:5,7,9,11 (blue), template size:3 with search size: 7, 9,11 (green), and template size: 5 with search size: 7,9,11,13 (red). (b) Computational time versus window size from Table I.

TABLE I  
CROSS-CORRELATION COEFFICIENT (CC) VALUES

| Template size (voxels) | Search size (voxels) | Mean CC | Computational Cost (mins) |
|------------------------|----------------------|---------|---------------------------|
| 3                      | 5                    | 0.9992  | 0.2857                    |
| 5                      | 7                    | 0.9968  | 3.3988                    |
| 7                      | 9                    | 0.9941  | 18.9051                   |
| 9                      | 11                   | 0.9910  | 72.7439                   |

TABLE II  
MEAN RADIAL STRAIN OF ANTERIOR-SEPTUM SEGMENT

| ID     | Volume (ml) | $\lambda_0$ | Iteration of Filtering | Set 1 Mean (%) | Set 2 Mean (%) |
|--------|-------------|-------------|------------------------|----------------|----------------|
| AP0007 | 108.16      | 6           | 6                      | 4.90±0.02      | 8.76±0.02      |
| AP0020 | 89.53       | 10          | 10                     | 4.75±0.01      | 8.43±0.01      |
| AP0093 | 141.83      | 10          | 10                     | 4.99±0.02      | 6.73±0.03      |
| AP0216 | 160.12      | 10          | 10                     | 4.91±0.03      | 6.65±0.05      |
| AP0224 | 93.60       | 6           | 6                      | 2.16±0.01      | 3.91±0.03      |
| AP0280 | 82.60       | 6           | 6                      | 12.83±0.05     | 14.99±0.07     |
| AP0490 | 77.84       | 10          | 10                     | 3.57±0.03      | 4.55±0.04      |
| AP0562 | 109.64      | 8           | 8                      | 4.98±0.03      | 6.29±0.03      |
| AP0574 | 89.77       | 10          | 10                     | 3.90±0.03      | 6.95±0.03      |
| AP0575 | 141.79      | 10          | 10                     | 5.88±0.03      | 6.40±0.03      |

Set 1: Template size: 5 voxels, Search size: 7 voxels  
Set 2: Template size: 7 voxels, Search size: 9 voxels

## IV. DISCUSSION

### A. Anisotropic Diffusion

Anisotropic diffusion smoothes and reduces image noise in the myocardial regions before 3D speckle tracking is performed. As shown in Fig. 2(c), the radial strains were underestimated without denoising. All segments had higher strain when we increased the  $\lambda_0$  parameter. However, for the largest smoothing parameter value  $\lambda_0 = 15$ , it is quite clear that the strain was overestimated in the posterior segment (blue line). Its strain values approach 30% and deviate significantly from the other segments. This is likely due to the fact that the speckle tracking is no longer tracking the myocardium properly on over-smoothed data with initial low contrast.

The optimal initial gradient threshold for each dataset varied and depended on the noise level. Since this filter theoretically regards structures with  $|\nabla I| > \lambda$  as edges, the experimental result is consistent with the theoretical investigation. The optimal  $\lambda_0$  correlated directly with the average magnitude of the gradient in the background speckle noise. The optimal initial threshold values were in the range 6-10 for our 10 COPD datasets as reported in Table II.

### B. 3D Speckle Tracking

The template window size must be selected such that it is small enough to enforce the assumption of simple translational displacements robust to noise. With small template sizes, cross-correlation coefficient values improved and computational cost decreased, but the radial strain measures were relatively low as the speckle tracking was not able to properly track the motion of the myocardium (top row) in Fig. 5(a). On the other hand, the larger template sizes, which resulted in lower CC values and longer computation times, tracked the myocardium more accurately and thus returned more consistent strain temporal profiles as displayed in (bottom row Fig. 5(a)). Furthermore, the example of the tracking motion illustrated in the short axis views in Fig. 5(c) confirmed that the tracking motions from

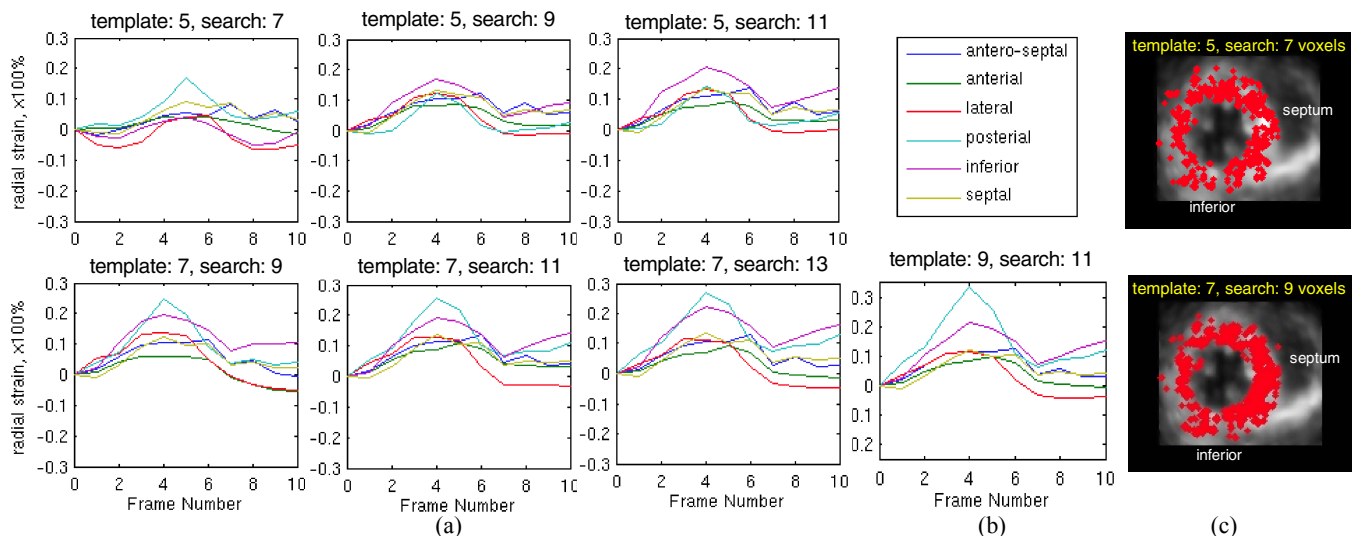


Fig. 5 : Examples of the temporal profiles of the radial strains (a) for fixed pre-processing parameters,  $\lambda_0 = 10$ , and with varying template and search sizes. (top row) Template size: 5 voxels with search size: 7, 9 and 11 voxels. (bottom row) Template size: 7 voxels with search size: 9, 11 and 13 voxels. (b) Largest window size: 9-voxel template and 11-voxel search. Short axis views (c) of the tracking motion for 5-voxel template with 7-voxel search (top) and 7-voxel template with 9-voxels search.

small template sizes (5 voxels) were less uniform than with larger template sizes (9 voxels).

In summary, small template windows are not effective for the myocardial motion tracking. Large window sizes suffer from higher computational costs and can introduce false positive matches. In our experimental investigation, the optimal template size was around 7 voxels and the optimal search size was around 9 voxels for the example data set in Fig. 5 (voxel size around 0.42-0.77 mm).

## V. CONCLUSION

Automated cardiac analysis on real-time volumetric ultrasound images has been increasingly required to improve and expand diagnostic abilities for cardiac functions. In our framework, we have developed the semi-automated LV strain analysis system using anisotropic diffusion to smooth images in the pre-processing stage, and we applied the 3D speckle tracking to extract the wall motion deformations. In this study, the influence of key parameters in the framework were investigated on the RT3D ultrasound images of 10 COPD patients. The findings in this study can serve as a guideline for the future application of our framework in 4D myocardial motion analyses.

## ACKNOWLEDGMENT

The authors would like to thank Eiichi Hyodo, Yukiko Oe, Aylin Tugcu, Shinichi Iwata and Frances Munoz for their help in the acquisition and analysis of the clinical ultrasound data. The authors would also like to thank Bruce McDermott and Betty Tsai at Siemens AG for providing us technical assistance with the SC2000 ultrasound machine.

## REFERENCES

- [1] V. L. Roger, A. S. Go, and D. M. Lloyd-Jones, "Heart disease and stroke statistics-2011 update: A report from the American Heart Association," *Circul.*, vol. 123, no. 4, pp. e18-e19, 2011.
- [2] L. N. Bohs, B. Geiman, M. Anderson, S. Gebhart, and G. E. Trahey, "Speckle tracking for multidimensional flow estimation," *Ultras.*, vol. 38, pp. 369-375, 2000.
- [3] B. H. Amundsen, T. Helle-Valle, T. Edvardsen, H. Torp, J. Crosby, E. Lyseggen, A. Støylen, H. Ihlen, J. A. Lima, O. A. Smiseth, and S. A. Slørdahl, "Noninvasive myocardial strain measurement by speckle tracking echocardiography: Validation against sonomicrometry and tagged magnetic resonance imaging," *J. Amer. Coll. of Cardiol.* vol. 47, no. 4, pp. 789-793 21 February 2006.
- [4] J. Crosby, B. H. Amundsen, T. Hergum, E. W. Remme, S. Langeland, and H. Torp, "3-D Speckle Tracking for Assessment of Regional Left Ventricular Function," *Ultra. in Med. & Biol.*, vol. 35, no. 3, pp. 458-471, March 2009.
- [5] Q. Duan, E. Angelini, O. Gerard, S. Homma, and A. Laine, "Comparing optical-flow based methods for quantification of myocardial deformations on RT3D ultrasound," in *IEEE Int. Symp. on Biomed. Img (ISBI)*, pp. 173-176, 2006.
- [6] Q. Duan, K. M. Parker, A. Lorsakul, E. D. Angelini, E. Hyodo, S. Homma, J. W. Holmes, and A. F. Laine, "Quantitative Validation of Optical Flow Based Myocardial Strain Measures Using Sonomicrometry," in *Proc. IEEE Int. Symp. on Biomed. Img (ISBI)*, Boston, USA, 2009.
- [7] Q. Duan, E. Angelini, S. Homma, and A. Laine, "Validation of Optical-Flow for Quantification of Myocardial Deformations on Simulated RT3D Ultrasound," in *2007 IEEE Int. Symp. on Biomed. Img*, Arlington, Virginia, 2007, pp. 944-947.
- [8] Q. Duan, E. D. Angelini, A. Lorsakul, S. Homma, J. W. Holmes, and A. F. Laine, "Coronary Occlusion Detection with 4D Optical Flow Based Strain Estimation on 4D Ultrasound," in *Proc. Func. Img & Model. of the Heart (FIMH)*, Nice, France, pp. 211-219, 2009.
- [9] A. Lorsakul, Q. Duan, M. Po, E. Hyodo, Y. Wang, S. Homma, and A. F. Laine, "Pipeline for the Quantification of Cardiac Strain Based on Optical Flow using 4D Ultrasound Data," presented at the Proc. of Northeast Bioengineering Conf. (NEBEC 2010), New York, NY, USA, 2010.
- [10] Q. Duan, E. D. Angelini, and A. Laine, "Assessment of fast anisotropic diffusion and scan conversion of real-time three-dimensional spherical ultrasound data for visual quality and spatial accuracy," in *SPIE Int. Symp. on Med. Img*, San Diego, CA, USA, pp. 331-342, 2004.
- [11] Y. Yu and S. T. Acton, "Speckle reducing anisotropic diffusion," *IEEE Trans. on Img Processing*, vol. 11, no. 11, pp. 1260-1270, November 2002.
- [12] J. Weickert, B. M. t. H. Romeny, and M. A. Viergever, "Efficient and reliable schemes for nonlinear diffusion filtering," *IEEE Trans. on Img Processing*, vol. 7, no. 3, pp. 398-410, 1998.
- [13] J. Montagnat, M. Sermesant, and H. Delingette, "Anisotropic filtering for model-based segmentation of 4D cylindrical echocardiographic images," *Pattern Recog. Letters*, vol. 24, pp. 815-828, 2003.
- [14] M. Cerqueira, N. Weissman, V. Dilsizian, A. Jacobs, S. Kaul, W. Laskey, D. Pennell, J. Rumberger, T. Ryan, and M. Verani, "Standardized myocardial segmentation and nomenclature for tomographic imaging of the heart," *Circul.*, vol. 105, pp. 539-542, 2002.
- [15] Q. Duan, E. Angelini, S. Herz, C. Ingrassia, O. Gerard, K. Costa, J. Holmes, and A. Laine, "Dynamic cardiac information from optical flow using four-dimensional ultrasound," in *IEEE Eng. in Med. & Biol. Soc. (EMBS)*, Shanghai, China, pp. 4465 - 4468, 2005.
- [16] Q. Duan, E. D. Angelini, S. L. Herz, C. M. Ingrassia, K. D. Costa, J. W. Holmes, S. Homma, and A. F. Laine, "Region-Based Endocardium Tracking on Real-Time Three-Dimensional Ultrasound," *Ultras. in Med. & Biol.*, vol. 35, no. 2, pp. 256-265, 2009.